

Supporting Information. Daniel Fink, Tom Auer, Alison Johnston, Viviana Ruiz-Gutierrez, Wesley M. Hochachka, and Steve Kelling. 2020. Modeling avian full annual cycle distribution and population trends with citizen science data. *Ecological Applications*.

Appendix S6: Estimating Local Trends

To estimate the average annual rate of change in a species' relative abundance with moderately high spatial resolution (25.2km x 25.2km) we used a two-step approach that exploits the ensemble structure of AdaSTEM. In the first step, hypothesis tests utilize the variation across the ensemble to filter out regions where base model estimates of the trend direction were inconsistent. We call this step the *signal filter*. Then in the areas that passed the signal filter, we averaged across the ensemble to estimate the average per year change in population size relying on the averaging to control the intra-ensemble variation.

In the first step of the signal filter, the direction of the slope for the log-linear regression of relative abundance on year are estimated for all locations in all base models. Then, at each location, a hypothesis test is conducted to determine if the trend is increasing or decreasing. Formally, let $\beta_{s,k}$ be the slope estimated at spatiotemporal location s , a single location in the 25km spatial grid, for base model $k, k = 1, \dots, N_s$, where N_s is the ensemble support, the number of overlapping base model estimates at location s . The slope parameter $\beta_{s,k}$ describes the average annual rate of change as the percent change per year in relative abundance. To test the direction of the slope, we use a very similar approach to that used to estimate AOO (See Appendix S5). Let $D_s = \sum d_{s,k}$ where $d_{s,k} = I(\beta_{s,k} > 0)$ indicates the direction of the trend. We model $D_s \sim \text{Binomial}(N_s, \delta_s)$ where δ_s is the probability of an increasing trend at location s .

When the trend is consistently estimated to be increasing across base models, δ_s will have values close to 1, and when the trend is consistently estimated to be decreasing it will have values close to 0. To infer when trends are consistently increasing and decreasing we conduct both one-sided binomial tests $H_0: \delta_s < 0.5$ and $H_0: \delta_s > 0.5$. Because species ranges often encompass many locations across the 25km grid, a large number of tests may be conducted. In order to identify as many locations with non-zero trends as possible while still maintaining a low false positive rate, we used FDR with $q = 0.01$.

Finally, we computed the ensemble averaged estimate of the trend. Like the first step, the trend was estimated as the slope here τ_s , at location s , from the log-linear regression of the relative abundances on years 2007-2016. Unlike the first step, the regression was fit using the ensemble average estimates of relative abundance, as described in the Estimating Occurrence and Relative Abundance Section.

We performed a subsampling analysis to assess the uncertainty associated with sampling variation across all the steps involved in estimating local trends. Because each of the base models was trained independently using independently subsampled data sets, sampling variation of the relative abundance estimates is captured among the base model estimates. Thus, to assess the uncertainty of the trend estimates, we computed 500 replicate ensemble trend estimates, each based on a random sample of 25 out of the 100 available base models. Unlike the subsampling procedure used to estimate uncertainty for the occurrence and abundance estimates (Appendix S4), we chose *not* apply any sample size corrections to produce conservative estimates of uncertainty.

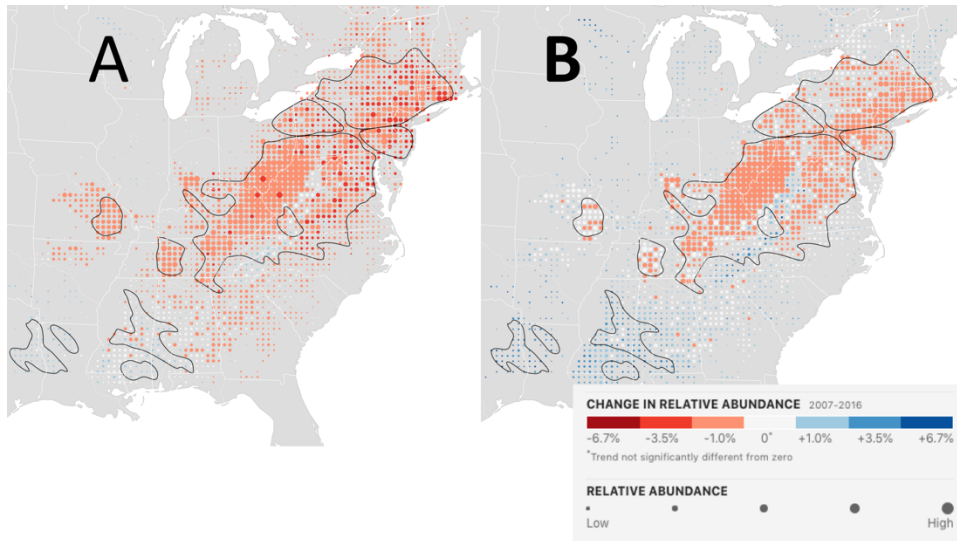


Figure S1: Wood Thrush 97.5% upper and 2.5% lower bound breeding season trend maps.

The maps show the location-wise (A) 97.5% upper and (B) 2.5% lower limits for the average percent change per year in relative abundance from 2007–16 during the breeding season (May 30– July 3). Each dot on the map represents a 25km x 25km area. To help visualize the relative change in population size at each location, the size of each dot has been scaled according to the average abundance at that location during the 10-year study period. The black contour lines delineate those regions across which the expected False Discovery Rate is at most 5% when identifying locations with increasing and decreasing trends.

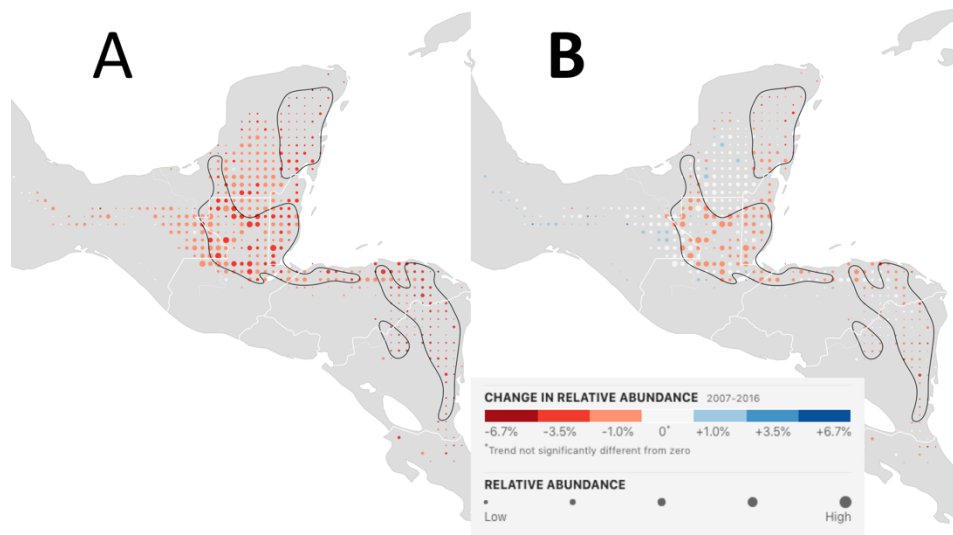


Figure S2: Wood Thrush 97.5% upper and 2.5% lower bound nonbreeding season trend maps. The maps show the location-wise (A) 97.5% upper and (B) 2.5% lower limits for the average percent change per year in relative abundance from 2007–16 during the breeding season (Dec 1–Feb 28). Each dot on the map represents a 25km x 25km area. To help visualize the relative change in population size at each location, the size of each dot has been scaled according to the average abundance at that location during the 10-year study period. The black contour lines delineate those regions across which the expected False Discovery Rate is at most 5% when identifying locations with increasing and decreasing trends.